 doi:10.20944/preprints202206.0216.v1

Article

Smart Systems for Material and Process Designing in Direct Nanoimprint Lithography Using Hybrid Deep Learning

Yoshihiko Hirai[1,2]*, Sou Tsukamoto[2], Hidekatsu Tanabe[2], Kai Kameyama[1], Hiroaki Kawata[1,2] and Masaaki Yasuda[1,2]

[1] Physics and Electronics Engineering, Graduate School of Engineering, Osaka Metropolitan University; y_hirai@omu.ac.jp
[2] Physics and Electronics Engineering, Graduate School of Engineering, Osaka Prefecture University; hirai@pe.osakafu-u.ac.jp
* Correspondence: y_hirai@omu.ac.jp; Tel.: (+81-72-254-9267)

Abstract: A hybrid smart process and material design system for nanoimprinting is proposed, which is combined with a learning system based on experimental and numerical simulation results. Instead of carrying out extensive learning experiments for various conditions, the simulation learning results are partially complimented when the results can theoretically be predicted by numerical simulation. In other words, the data that are lacking in experimental learning are complimented by simulation-based learning results. Therefore, the prediction of nanoimprint results without experimental learning could be realized under various conditions, even for unknown materials. In this study, material and process designs are demonstrated for a low-temperature nanoimprint process using glycerol-containing polyvinyl alcohol. The experimental results under limited conditions were learned, to investigate optimum glycerol concentrations and process temperatures. Simulation-based learning was used to predict the dependence on press pressure and shape parameters. The prediction results for unknown glycerol concentrations agreed well with the follow-up experiments.

Keywords: direct nanoimprint; process design; deep learning

1. Introduction

In conventional photo lithography, nanostructures are obtained by processing photosensitive materials. On the other hand, nanoimprint lithography [1,2] directly achieves nanofabrication on various materials, for example, organic semiconductors [3-5], low-melting-point glass, etc. [6-8]. This enables various applications in electronics, photonics and biodevices, which have been difficult to realize using conventional lithography.
Both optimum process design and defect elimination are common issues. In conventional lithography, computational lithography has significantly improved for process design. Attempts have also been made to use artificial intelligence to predict defect locations (hotspots) and optimize layout. A successful reason for this is that the use of highly standardized materials and equipment make it suitable for deep learning systems based on huge databases and optimizing pattern layouts that are realized to eliminate defects [9-12].

On the other hand, the process conditions are determined by mechanical properties such as the viscoelastic modulus of the material and topological conditions such as pattern width, pattern height and pressure [13-16] in nanoimprint lithography. Therefore, the process conditions are determined by simulation analysis and empirical knowledge based on measurements of mechanical properties and topological conditions [17]. One feature of nanoimprinting is the use of application-specific materials. This requires optimization of the process, including pattern layout, according to the material's properties.

 doi:10.20944/preprints202206.0216.v1

However, for materials with unknown properties or new processes, it is necessary to carry out a series of preliminary experiments, measure the material properties and accumulate nanoimprinting results, which means that process and material optimization takes an enormous amount of time.

The aim of this study was to propose a smart manufacturing system that provides an optimized process for a wide variety of materials and structures using an artificial neural network system [18-20] that can handle novel processes and materials based on a knowledge base of experiments and simulations.

2. Low-temperature direct nanoimprint for Polyvinyl Alcohol (PVA) with Glycerol Additives

The aim of this study is to develop a low-temperature, direct nanoimprint process for PVA, which is a water-soluble polymer and has great value for its use as a disposable mold and sacrificial layer. However, the water solubility of PVA is impaired when heated above about 150℃. Therefore, the process temperature should be below 150℃. However, higher pressing pressure is needed, and this causes defects in the process.

To solve this problem, we found that the pressing temperature of PVA can be lowered by adding glycerol to PVA. Figure 1 demonstrates the direct nanoimprint to glycerol-added PVA. The effect of glycerol additive is evidently revealed.

However, there is no easy way of finding the optimal additive concentration of Glycerol, and many investigation experiments are required to confirm the optimal conditions by successively changing the amount of Glycerol that is added and the process temperature. On the other hand, for process simulation, the material parameters, such as elastic modulus for thin film, should be measured.

Therefore, we attempted to construct an optimization system for nanoimprint materials and their processes using artificial intelligence.

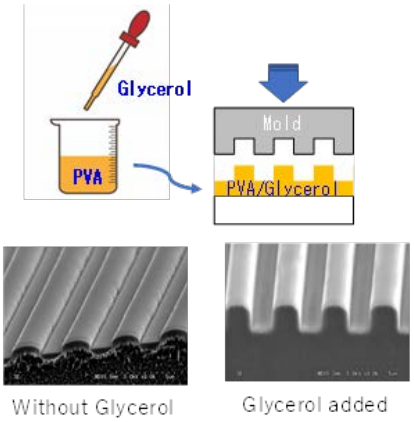

Figure 1. Direct nanoimprint results with and without glycerol additives to PVA. (10MPa, 130℃, Line width=2.0μm).

3. Hybrid deep-learning system for nanoimprint material and process

To realize a smart design system for nanoimprint materials and processes, we propose a novel system to predict the pattern height after thermal nanoimprinting by learning based on experimental data and numerical simulation data, where the simulation learning

Preprints (www.preprints.org) | NOT PEER-REVIEWED | Posted: 15 June 2022 doi:10.20944/preprints202206.0216.v1

complements the learning results, which could not be carried out in experiments. We refer to this system as a hybrid system, which combines learning from experiments with learning from numerical simulations. Figure 2 shows the system diagram. The input parameters are process conditions such as pressure and temperature, material characteristics such as solvent concentration, and topological structure such as pattern size and feature for each learning system. In this case, the output is the pattern height after nanoimprinting.

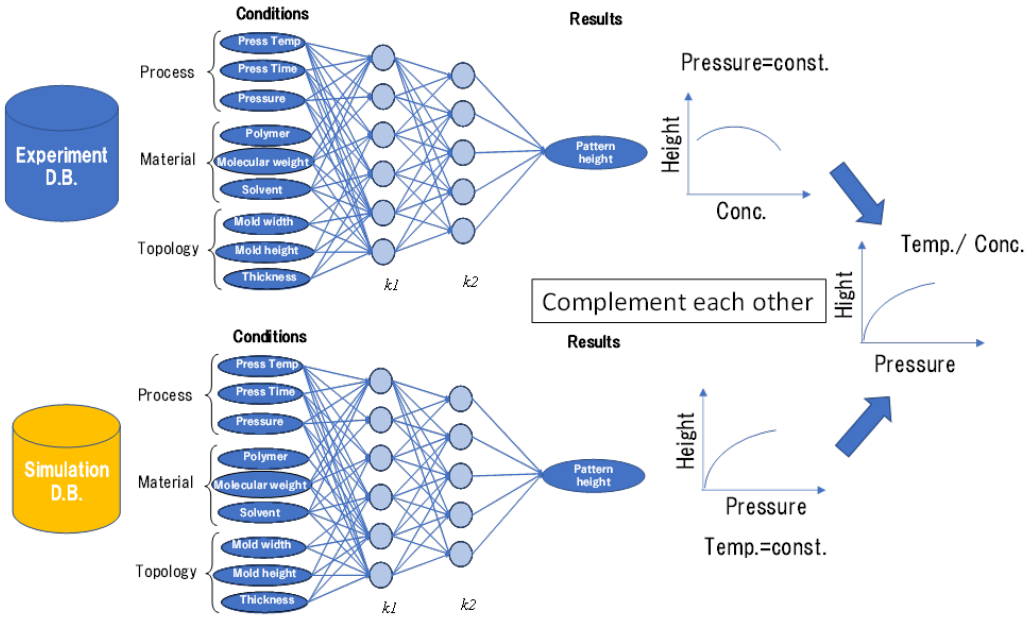

Figure 2. Schematics of 'hybrid' deep learning system in combination with experiment and simulation.

In experimental learning, the learning data were extracted by varying the process conditions by variations in the Glycerol concentration and process temperature. Therefore, topological conditions such as mold groove width or depth and process conditions such as pressing pressure were fixed to minimalize the number of experiments.

In the simulation learning, simulation results under some representative conditions were used for learning, where the data were extracted using polymethyl methacrylate (PMMA) as a reference material instead of using actual material. The importance of this is that the nanoimprinted results were reported in our simulation and experimental studies [13-15], where the results were determined by the relative pressure on the modulus of the material and the topology of the mold based on the similarity laws of the continuum mechanics.

The simulation learning could calculate dependencies on pattern shape, press temperature, press pressure and the elastic modulus of the material, but could not handle dependencies on unknown materials for which the physical parameters were unknown. As system is a normalization system based on continuum mechanics. Under the law of similarity, the relative value of the normalized pattern height can be derived from the normalized pressure P/E, where P is the press pressure and E is the modulus of the material.

In other words, if the mechanical properties of the polymers are relatively the same, the normalized relative press pressure can be obtained if the normalized pattern height is known. As a result, the relative pressure can be estimated even if the elastic modulus of the material is unknown.

 doi:10.20944/preprints202206.0216.v1

Furthermore, if the relative press pressure is known, the pattern height after nanoimprinting can be predicted by changes in the press pressure.

Thus, under certain approximations, simulation can complement the learning results.

In this study, PVA with glycerol was considered a rubber elastic material and the Mooney–Rivlin model was used to represent the mechanics, with the Mooney coefficient determined by using a well-known empirical formula [21,22].

From these learning results, the optimum concentration of glycerol could be designed and process conditions could be proposed to obtain the required pattern.

In the experimental learning, the dependence of pattern height on glycerol concentration and press temperature is predicted. However, the dependence on press pressure could not be predicted because the learning data were not taken into account.

The elastic modulus of PVA with Glycerol was substituted for that of polymethyl methacrylate (PMMA). According to the similarity rule, it was assumed that the pattern shape after nanoimprinting is uniquely determined by the relative values P/E of the pressing pressure P and the elastic modulus E, as described above.

Thanks to this approximation, the measurement of the actual elastic modulus of each polymer is omitted and the relative relationship of the pattern height to the press pressure can be obtained. The same can be applied to changes in mold topography.

For deep learning, a multi-layer back-propagation neural network (BPNN) system, which is one of the most representative deep learning systems among machine learning systems, is used to predict the nanoimprinting results and propose nanoimprinting processes and materials. The system is a homemade system using Python [23] convened with Microsoft Excel [24]. Both learning systems consist of two hidden layers of 11 nodes that consider the prediction error. The typical learning coefficient was set to 0.01 and the number of learning epochs was around 5,000 or more, which takes several hours using conventional personal computers without a normal Graphics Processing Unit (GPU).

4. Results and Discussions

4.1. Characterization of PVA containing glycerol and prediction of pattern formability

First, the pattern formability of glycerol-containing PVA was experimentally investigated. Here, the nanoimprinted result is simply characterized as the pattern height after nanoimprinting.

Table 1 shows our previous experimental results [20] of the cross-section images of the pattern after nanoimprint. In this experiment, the weight concentration of Glycerol was varied from 0 to 25%. The pressing temperatures were 100, 130, and 150°C. The press temperatures were 100°C, 130°C and 150°C. The press pressure was 10 MPa, the line width of the pattern was 2 μm, the groove depth of the mold was 2 μm and the thickness of the PVA was 3 μm, respectively.

The nanoimprinting was performed at least three times under each condition, for a total of 43 experiments. These were used as learning data.

Figure 3 shows the average height of the patterns under each condition. It is difficult to visually extract the regularity from the graph.

In the learning process, we determine the weight function of the neural networks as described in Fig.3 for an experimental learning system. About 70% of the experimental data were used as training data to learn the relationship between glycerol concentration, process temperature, and pattern height after nanoimprinting.

Table 1. The scanning electron microscope (SEM) images of experimental results for PVA with glycerol (pressure:10MPa, 2.0μm line and space).

Preprints (www.preprints.org) | NOT PEER-REVIEWED | Posted: 15 June 2022 doi:10.20944/preprints202206.0216.v1

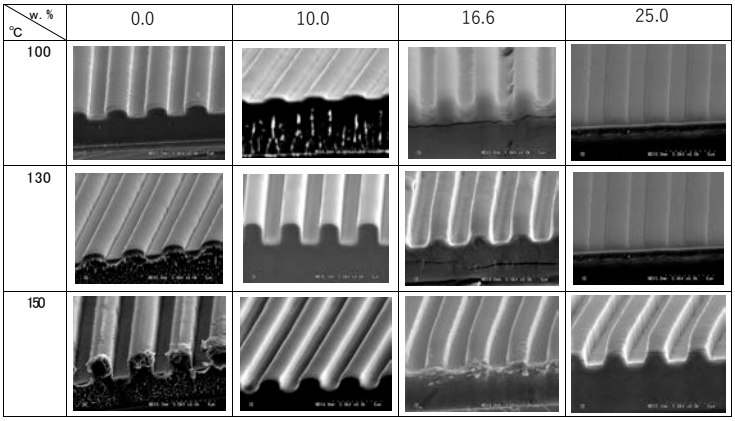

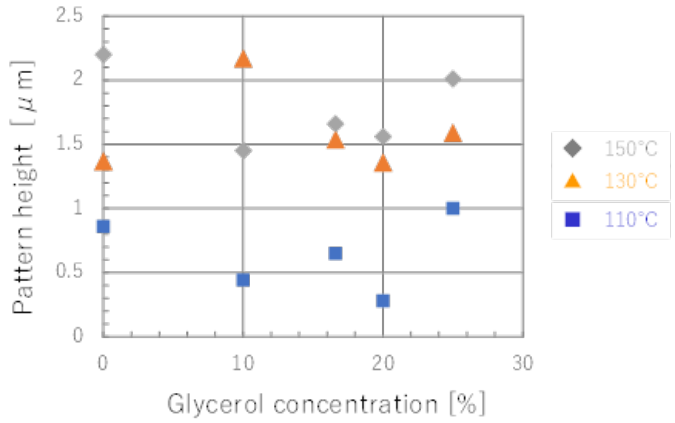

Figure 3. Experimental results for learning data at various glycerol concentrations under limited process condition.

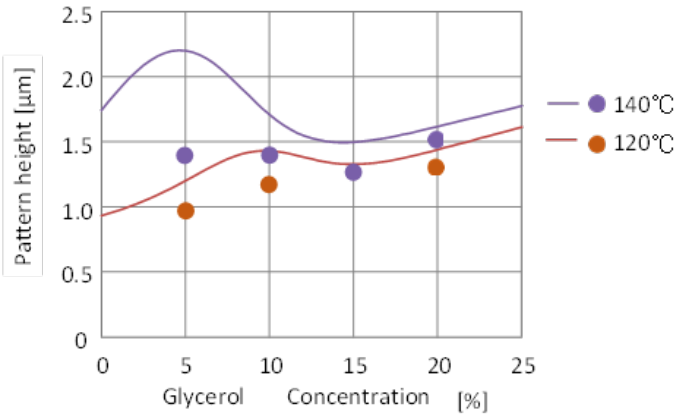

Figure 4. Predicted pattern height (solid lines) and verification experimental results (dots) for various Glycerol concentration at 120℃ and 140℃ based on experimental learning data at 110℃, 130 ℃ and 150℃.

Figure 4 shows the results of predicted pattern height at temperatures not present in the learning experimental data, with solid lines.

The dots in the figure show the experimental results.

Preprints (www.preprints.org) | NOT PEER-REVIEWED | Posted: 15 June 2022 doi:10.20944/preprints202206.0216.v1

On the other hand, the predicted values at a glycerol concentration of 5% and a press temperature of 140°C deviate from the experimental values. This is presumably due to overestimation, influenced by the results at a 0% glycerol concentration and 150°C. However, at other concentrations and temperatures, the predictions are generally successful at predicting the experimental results.

Based on the learning results (weight function), we predicted the dependence of the glycerol concentration on varying process temperatures.

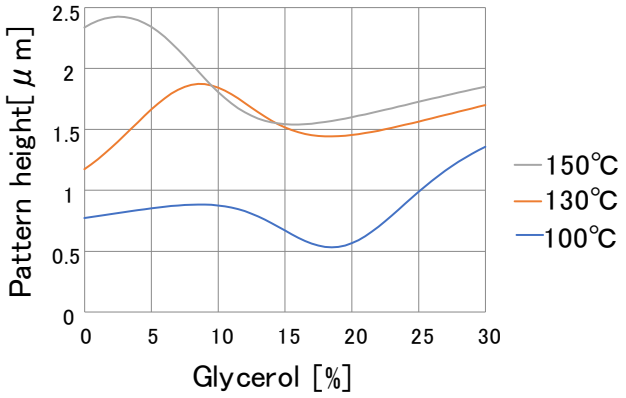

Figure 5. Predicted pattern height (solid lines) in various glycerol concentration based on experimental learning data.

Figure 5 shows the prediction results. In various temperature, the pattern height has local peck around 10% of the glycerol concentration. It can be predicted that a 10% glycerol concentration and a press temperature that is as low as possible, around 130°C will more effectively improve pattern formability.

Based on deep learning, the pattern height after nanoimprinting could be predicted with a constant pressure, arbitrary temperature and glycerol concentration.

However, pressure dependence was not included because it was not considered in the learning experiments.

4.2. Pattern height prediction by simulation-based learning

To predict the pattern shape after nanoimprinting in relation to the mold shape, polymer topography and press pressure, a learning system is constructed to predict the pattern height using deep learning from representative shape conditions and relative pressure conditions, learned in advance by simulation.

First, a comparison was made between simulation and experiment. Here, the deformation state of PMMA was compared using a rubber elastic body model. The Young's modulus E of PMMA at the pressing temperature was measured beforehand, and the results of the experiment and simulation are shown when PMMA was pressed at a relative pressure P/E to the pressing pressure P. Although the two are not in perfect agreement, they are in a relative general agreement, and the simulation confirms that the formability can be predicted to some extent.

Next, to prepare the learning data, the relationship between the aspect ratio of the mold grooves and the height of the pattern when the relative pressing pressure was varied was investigated by simulation.

Preprints (www.preprints.org) | NOT PEER-REVIEWED | Posted: 15 June 2022 doi:10.20944/preprints202206.0216.v1

Table 2 shows some examples of the results. Here, the initial polymer film thickness was set to three times the mold groove depth, and the aspect ratio (groove depth/width) of the mold groove structure was varied.

Table 2. Simulation results for learning data.

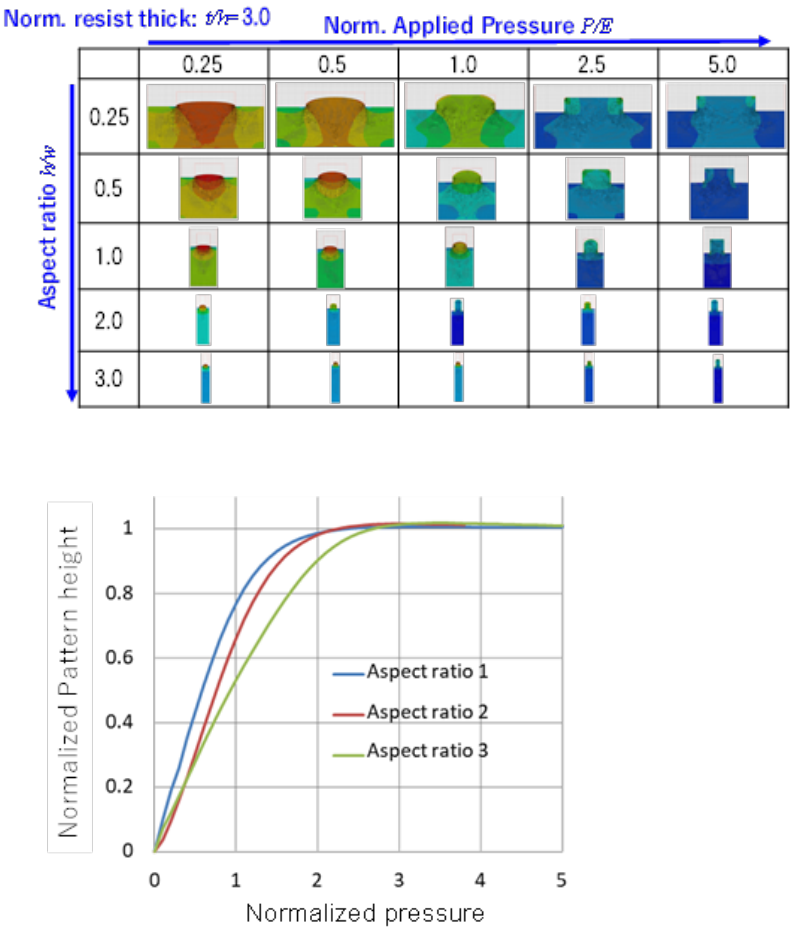

Figure 6. Prediction results of the pattern height after nanoimprinting for mold patterns with various aspect ratios, varying with applied pressure using deep learning.

Figure 6 shows the prediction results of the pattern height after nanoimprinting for mold patterns in various aspect ratios, with varying levels of applied pressure, by deep learning using simulation results as learning data. Due to the prediction accuracy, the results are partly crossed in detail, but this is not a fatal issue with regard to the objective of predicting rough results. What is important is that the system determines the weight function in neural networks, and deep learning provides the pattern height after nanoimprinting under arbitrary process conditions without a fudge computational cost of numerical simulation.

4.3. Hybrid system for material and process design for nanoimprinting

We have demonstrated a system for learning pattern heights when varying Glycerol concentration in PVA and process temperature with a fixed press pressure and mold topography, and a system for learning and predicting nanoimprinting results for variations in press pressure and pattern topography, complementing the simulation-based learning.

The former system uses learning data based on experiments, while the latter system uses simulation results using PMMA as a representative reference polymer as learning data.

Preprints (www.preprints.org) | NOT PEER-REVIEWED | Posted: 15 June 2022 doi:10.20944/preprints202206.0216.v1

As the results of nanoimprinting are mostly determined by the mechanical property of the polymer, i.e., the elastic modulus or viscoelasticity of the polymer, according to the law of similarity, the PVA containing glycerol behaves in a similar way to those of reference polymers, such as PMMA, with an equivalent relative modulus of the polymer.

In other words, if the relative press pressure is equivalent to the modulus of elasticity of the polymer, the nanoimprinting results will be the same.

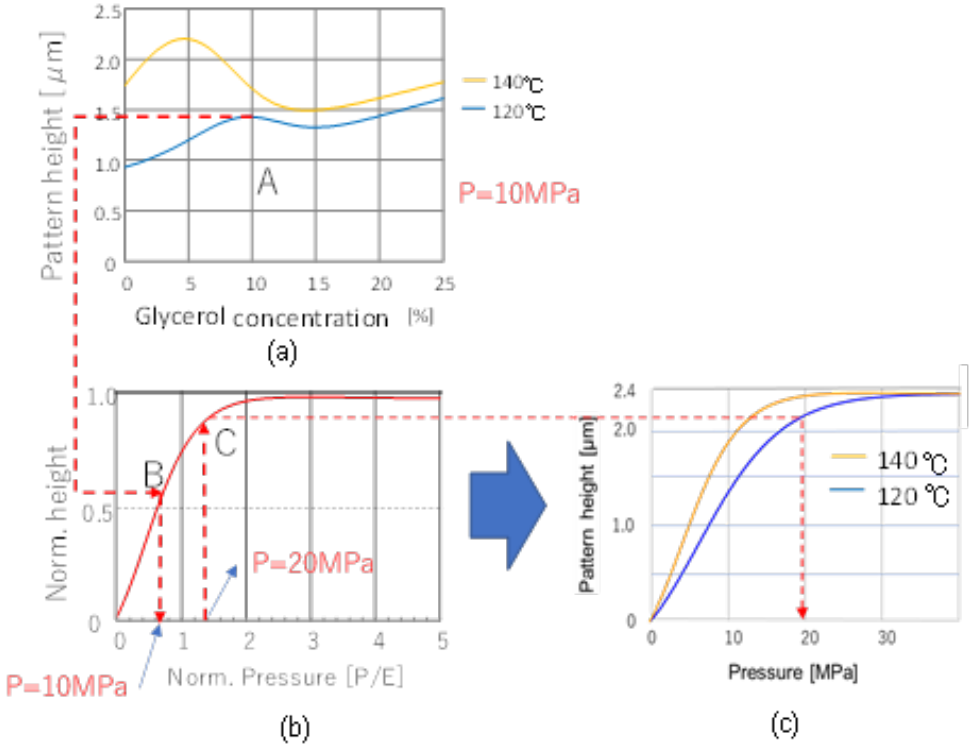

Figure 7. Diagram of procedure for prediction by hybrid learning system.

The procedure of the prediction is shown in Fig. 8 for glycerol-containing PVA.

First, we chose the glycerol concentration, referring to Fig. 4. For instance, when the press temperature was set to 120 ℃, we chose 10% as the pattern height with a local peak (A in Fig.7a).

The pattern height was predicted to be approximately 1.4 μm. This height corresponds to a relative height of approximately 0.6, where the mold depth is 2.3 μm.

Next, we predict pattern height for various nanoimprinting pressures at 120 ℃. The learning results from the simulation were used to predict the relationship between the pressure and nanoimprinting height for the relative aspect ratio of 1.15, as shown in Fig. 7b. The relative press pressure (P/E) for a relative height of 0.6 can be read from the graph as approximately 0.65 (B in Fig.7b); namely, the experimental pressing pressure of 10 MPa for PVA could be regarded as pressing at a relative pressure of 0.65.

Therefore, the nanoimprinting result when pressed at, for example, 20 MPa, can be traced at a relative pressure of 1.3 (C in Fig.7c), which is twice the relative pressure at 10MPa.

This operation can be automatically charted by a macro-program such as Excel, based on the results of deep learning predictions.

In this way, the relationship between the actual pressing pressure and the nanoimprinting height can be linked and predicted under mostly material, process and topology conditions.

 doi:10.20944/preprints202206.0216.v1

As a result, experimental results with missing pressure and geometry conditions could be complemented by learning simulation results based on similarity rules to predict nanoimprint results. This minimizes the amounts of learning data needed for unknown materials with many parameters to be varied.

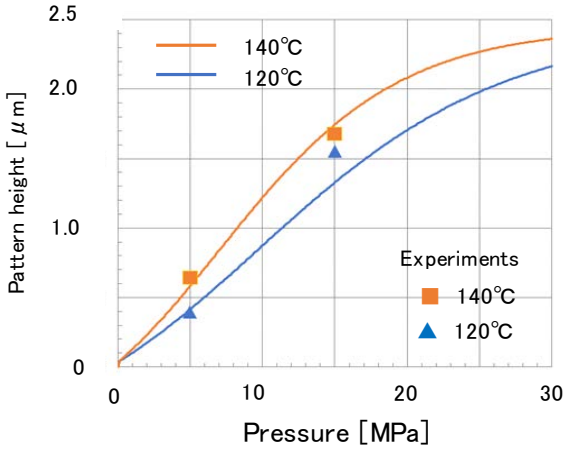

Figure 8. Prediction of pattern height with varying pressure by hybrid deep learning and experimental results. The nanoimprinting temperature was 120℃ and 140℃ and the glycerol concentration was 10%.

Figure 8 shows the predicted results and follow-up experimental results for various pressures at a nanoimprint temperature of 120°C and 140°C and glycerol concentration of 10%. The solid line shows the pattern height predicted by hybrid learning, and the square and triangle show the experimental results at 5 MPa and 15 MPa, respectively. The deep learning predictions are in good agreement with the experimental results.

In summary, we proposed a system that combines deep learning from experiments to characterize material properties and deep learning from simulation results to predict formability under varying process conditions. It is shown that these systems can complement each other's learning results, enabling a rough prediction of nanoimprinting performance for unknown materials under unknown process conditions.

According to this approach, it is possible to predict optimal process and material conditions by learning multiple nanoimprint results for an unknown material, even without knowing the mechanical properties of the material that are important for nanoimprinting, namely the elastic modulus. This could be useful for direct nanoimprint process design.

The remaining issue will be verifying to what extent the similarity rule, which, in this case, treated the well-known PMMA as a standard material, can be adapted to other resin materials and functional materials.

5. Conclusions

We have proposed a smart design system for nanoimprinting processes and materials based on a hybrid learning system from experiments and numerical simulation results.

We believe that this smart system can provide a good prediction of results for unknown materials in direct nanoimprinting with diverse materials.

In future, the system will be extended to various materials and topological structures to confirm the results.

References

1. S. Chou, P. Krauss, and P. Renstrom, Imprint of sub-25 nm vias and trenches in polymers, *Appl. Phys. Lett.*,**1995**, 67, pp. 3114-3116, DOI: /10.1063/1.114851.
2. S. Chou, P. Krauss, and P. Renstrom, Nanoimprint lithography, *J. Vac. Sci. Technol*. B, **1996**, 14, pp. 4129-4133, DOI: /10.1116/1.588605.
3. M. Austin and S. Chou, Fabrication of 70 nm channel length polymer organic thin-film transistors using nanoimprint lithography, *Appl. Phys. Lett*., **2002**, 81, pp.4431-4433, DOI: /10.1063/1.1526457.
4. G. Leising, B. Stadlober, U. Haas, A. Haase, C Palfinger, H. Gold, and G. Jakopic, Nanoimprinted devices for integrated organic electronics, *Microelectronic Eng*., **2006**, 83, pp.831-838, DOI: /10.1016/j.mee.2006.01.241.
5. K. Tomohiro, N. Hoto, H. Kawata, and Y. Hirai, Fine Pattern Transfer of Functional Organic Polymers by Nanoimprint, *J. Photopolymer Sci. Technol*., **2011**, 24, pp.71-75, DOI: /10.2494/photopolymer.24.71.
6. M. Li, H. Tan, L. Chen, J. Wang, and S. Chou, Large area direct nanoimprinting of SiO_2-TiO_2 gel gratings for optical applications, *J. Vac. Sci. Technol. B*, 21, **2003**, pp. 660-663, DOI: /10.1116/1.1545736.
7. 7. Y. Hirai, K. Kanakugi, T. Yamaguchi, K. Yao, S. Kitagawa, and Y. Tanaka, Fine pattern fabrication on glass surface by imprint lithography, *Microelectronic Eng*., **2003**, pp.67-68, pp. 237-244, DOI: /10.1016/S0167-9317(03)00077-7.
8. Y. Hirai and Y. Tanaka, Application of nano-imprint lithography, *J. Photopolymer Sci. Technol*., **2002**, 15, pp. 475-480, DOI: /10.2494/photopolymer.15.475.
9. H. Yang, L. Luo, J. Su, C. Lin, and B. Yu, Imbalance aware lithography hotspot detection: a deep learning approach, *J. Micro/Nanolithography. MEMS, and MOEMS*, **2017**, 16, 033504, DOI: /10.1117/1.JMM.16.3.033504.
10. X. Ma, X. Zheng, and G. Arce, Fast inverse lithography based on dual-channel model-driven deep learning, *Optics Express*, **2020**, 28, pp.20404-20421, DOI: /10.1364/OE.396661.
11. T. Akter and S. Desai, Developing a predictive model for nanoimprint lithography using artificial neural networks, *Materials and Design*, **2018**, 160, pp.836–848, DOI: /10.1016/j.matdes.2018.10.005.
12. S. Aihara, N. Takakura, F. Kizu, S. Jimbo, K. Ishibashi, J. Seki, Y. Oguchi, T. Asano, Y. Matsuoka, M. Tamura, and O. Morimoto, Addressing NIL integration for semiconductor device manufacturing, Proc. SPIE, Novel Patterning Technologies, **2021**, 1161007, DOI: /10.1117/12.2584720.
13. Y. Hirai, M. Fujiwara., T. Okuno, Y. Tanaka, M. Endo, S. Irie, K. Nakagawa, and M. Sasago, Study of the resist deformation in nanoimprint lithography, *J. Vac. Sci. Technol. B*, **2001**, 19, pp. 2811-2815, DOI: /10.1116/1.1415510.
14. Y. Hirai, S. Yoshida, and N. Takagi, Defect analysis in thermal nanoimprint lithography, *J. Vac. Sci. Technol. B*, **2003**, 21, pp.2765-2770, DOI: /10.1116/1.1629289.
15. Y. Hirai, T. Konishi, T. Yoshikawa, and S. Yoshida, Simulation and experimental study of polymer deformation in nanoimprint lithography, *J. Vac. Sci. Technol. B*, **2004**, 22, pp.3288-3293, DOI: /10.1116/1.1826058.
16. Y. Hirai, Y. Onishi, T. Tanabe, M. Shibata, T. Iwasaki, and Y. Irie, Pressure and resist thickness dependency of resist time evolutions profiles in nanoimprint lithography, *Microelectronic Eng*., **2008**, 85, pp.842-845, DOI: /10.1016/j.mee.2007.12.084.
17. Y. Hirai, T. Yoshikawa, N. Takagi, and S. Yoshida, Mechanical properties of poly-methyl methacrylate (PMMA) for nano imprint lithography, *J. Photopolymer Sci. Technol*., **2003**, 16, pp. 615-620, DOI: /10.2494/photopolymer.16.615.
18. D. Specht, Probabilistic neural networks, Neural Networks, **1990**, 3, pp.109-118, DOI: /10.1016/0893-6080(90)90049-Q.
19. Y. LeCun, Y. Bengio, and G. Hinton, Deep learning, Nature, **2015**, 521, pp. 436-444, DOI: /10.1038/nature14539.

 doi:10.20944/preprints202206.0216.v1

20. S. Tsukamoto, H. Tanabe, R. Yamamura, K. Kameyama, H. Kawata, M. Yasuda, and Y. Hirai, Proposal of hybrid deep learning systems for process and material design in thermal nanoimprint lithography, *J. Photopolymer Sci. and Technol.*, **2021**, pp.145-148, DIO:/10.2494/photopolymer.34.145
21. M. Moony, A theory of large elastic deformation, *J. Appl. Phys.*, **1940**, 11, pp.582-592, DOI: /10.1063/1.1712836.
22. R. S. Rivlin, Large elastic deformations of isotropic materials IV. Further developments of the general theory, *Phil. Trans. Roy. Soc. London, Ser. A*, **1948**, 241, pp.379-397, DOI: /10.1098/rsta.1948.0024.
23. https://www.python.org/
24. https://www.microsoft.com/en-us/microsoft-365/microsoft-office/